Atorvastatin Therapy is Associated with Greater and Faster Cerebral Hemodynamic Response

Published in final edited form as:
Brain Imaging Behav. 2008 June 1; 2(2): 94. doi:10.1007/s11682-007-9019-7.

Atorvastatin therapy is associated with greater and faster cerebral hemodynamic response

Guofan Xu[1,2], **Michele E. Fitzgerald**[1,2], **Zhifei Wen**[2], **Sean B. Fain**[2], **David C. Alsop**[4], **Timothy Carroll**[3], **Michele L. Ries**[1,2], **Howard A. Rowley**[2], **Mark A. Sager**[2], **Sanjay Asthana**[1,2], **Sterling C. Johnson**[1,2], and **Cynthia M. Carlsson**[1,2]

[1] William S. Middleton VA Hospital, Madison, WI

[2] University of Wisconsin, Madison, WI

[3] Northwestern University, Chicago, IL

[4] Beth Israel Deaconess Medical Center and Harvard Medical School, Boston, MA

Abstract

Hypercholesterolemia in midlife increases the risk of subsequent cognitive decline, neurovascular disease, and Alzheimer's disease (AD), and statin use is associated with reduced prevalence of these outcomes. While statins improve vasoreactivity in peripheral arteries and large cerebral arteries, little is known about the effects of statins on cerebral hemodynamic responses and cognition in healthy asymptomatic adults. At the final visit of a 4-month randomized, controlled, double-blind study comparing atorvastatin 40 mg daily to placebo, 16 asymptomatic middle-aged adults (15 had useable data) underwent blood oxygen level dependent (BOLD) functional magnetic resonance imaging (fMRI), arterial spin labeling (ASL) quantitative cerebral blood flow (qCBF), dynamic susceptibility contrast (DSC) and structural imagings of the brain. Using a memory recognition task requiring discrimination of previously viewed (PV) and novel (NV) human faces, fMRI was used to elicit activation from brain regions known to be vulnerable to changes associated with AD. The BOLD signal amplitude (PV > NV) and latency to each stimulus were tested on a voxel basis between the atorvastatin (n=8) and placebo (n=7) groups. Persons randomized to atorvastatin not only showed significantly greater BOLD amplitude in the right angular gyrus, left superior parietal lobule, right middle temporal and superior sulcus than the placebo group, but also decreased hemodynamic response latencies in the right middle frontal gyrus, left precentral gyrus, left cuneus and right posterior middle frontal gyrus. However, neither the resting cerebral blood flow (CBF) measured with ASL nor the mean transit time (MTT) of cerebral perfusion calculated from DSC showed differences in these regions in either group. The drug related BOLD differences during memory recognition suggest that atorvastatin may have improved cerebral small vessel vasoreactivity, possibly through an effect on endothelial function. Furthermore, these results suggest that the effect of atorvastatin on the task-induced BOLD signal may not be a simple consequence of baseline flow change.

Keywords

BOLD; Hemodynamic response; Arterial Spin Labeling; Dynamic susceptibility Contrast; event-related fMRI; Alzheimer's Disease

Introduction

Functional magnetic resonance imaging (fMRI) with blood oxygenation level dependent (BOLD) contrast has been used to study cognitive abnormalities in people with Alzheimer's

disease (AD) and people at risk for AD (Smith et al., 1999; Petrella et al., 2003; Trivedi et al., 2006). This body of research suggests potential for fMRI in the early detection of AD (Fleisher et al., 2005; Johnson et al., 2006a) and the prediction of preclinical disease progression (Dickerson et al., 2005). Increasing evidence suggests that neuropathological changes occur in people at risk for AD well before the onset of measurable symptoms (Braak and Braak, 1991). Therefore, recent prevention research has focused on asymptomatic individuals at risk for AD due to a family history of the disease or the presence of other genetic or vascular risk factors (Sager et al., 2005).

Hypercholesterolemia in midlife is a risk factor for developing AD decades later (Kivipelto et al., 2002). Statins not only lower serum cholesterol levels, but also improve vasoreactivity in peripheral arteries and large cerebral arteries and are associated with a reduced prevalence of AD (Masse et al., 2005). However, little is known about the effects of statins on cerebral hemodynamic responses and cognition in asymptomatic persons at risk for AD.

Neuroimaging studies of people at risk for developing AD report either reduced BOLD signal (Johnson et al., 2006b) related to AD risk factors or increased signal attributed to putative compensatory phenomena (Bookheimer et al., 2000). The fMRI BOLD signal itself is sensitive to changes in baseline cerebral blood flow (CBF) and cerebral metabolism of oxygenation that tightly accompany focal neuronal activity (Hoge et al., 1999; Ogawa et al., 1990). For example, Cohen et al. showed that the magnitude and dynamic characteristics of the BOLD response in the visual cortex are a function of basal cerebrovascular conditions (Cohen et al., 2002). However, direct comparisons of the BOLD signal between groups or conditions rely on the assumption that the underlying neurovascular coupling is comparable. This assumption may not hold with the introduction of pathological changes or drug intervention effects in the brain. For example, an uncharacteristic BOLD signal was found in a patient with carotid artery stenosis during performance of a simple motor task (Rother et al., 2002). Furthermore, the normal aging process has been reported to affect the coupling of neural activity to the BOLD hemodynamic response (D'Esposito et al., 1999).

One way to address this limitation is to study the temporal course of hemodynamic response within individual subjects (Calhoun et al., 2004) in addition to the signal amplitude. By analyzing the temporal profile of the hemodynamic response, Miezin et al. found regional differences in the hemodynamic response latency peak within the same subject (Miezin et al., 2000). Henson et al. has introduced a computationally efficient method that can be applied to detect whole brain differences in the latency of hemodynamic responses (Henson et al., 2002). With this method, the temporal derivative of the model is used to estimate the amount and direction of latency shift (±1.78 s) to an assumed BOLD peak of 6 s following an event-related activity.

In this paper we applied the Henson et al. method to determine whether there were differences in BOLD signal amplitude or latency in persons randomized to atorvastatin 40 mg daily for 4 months compared to those assigned placebo. Because the hemodynamic response amplitude or latency difference could be caused by differences in cerebral perfusion across subjects (Laurienti et al., 2003), both cerebral blood flow (CBF) and mean transit time (MTT) values were measured with arterial spin labeling (ASL) and dynamic susceptibility contrast (DSC) MR imaging techniques, respectively. To further examine brain regions that are vulnerable to early structural and functional changes associated with AD (Petersen et al., 1997), fMRI was used with an event-related, episodic recognition memory task that was expected to elicit activation in parietal and frontal regions (Haxby et al., 1996).

Methods and Materials

Participants and experimental design

This randomized, double-blind, placebo-controlled trial was conducted using a protocol approved by the local Institutional Review Board. Written informed consent was obtained from all participants after the study procedures were fully explained. Sixteen asymptomatic, middle-aged adult children (ages 38–66 years) of persons with AD participated in this trial. Participants were recruited from the local community and the Wisconsin Registry for Alzheimer's Prevention (WRAP), a statewide registry of asymptomatic adult children (aged 40–65 years) of persons with probable or definite AD (Sager et al., 2005). Prior to enrollment, a diagnosis of definite or probable AD in one or both parents was confirmed using the National Institute of Neurological and Communicative Disorders and Stroke and Alzheimer's Disease and Related Disorders Association (NINCDS-ADRDA) criteria (McKhann et al., 1984) through clinical evaluation and/or chart review by physicians and neuropsychologists with expertise in the diagnosis of dementia. Study exclusion criteria included: current use of cholesterol-lowering medications; contraindications to statin therapy or MRI; history of dementia, major head trauma, or abnormal structural MRI.

The study was comprised of three visits: baseline, month 1, and month 4. At baseline, subjects were randomized in a 1:1 ratio to receive either atorvastatin 40mg daily (n=8) or matching placebo (n=8). Blood samples were collected at each visit after a 12-hour fast (lipid profile, high sensitivity C-reactive protein [hs-CRP], aspartate aminotransferase [AST], alanine aminotranferase [ALT], creatine kinase [CK], creatinine [Cr]). All samples were obtained at the University of Wisconsin General Clinical Research Center (GCRC) between August 2006 and April 2007 and were evaluated by a clinician for the presence of any potential side effects of the medication. At month 4, participants underwent a BOLD fMRI scan using a recognition memory task, quantitative cerebral perfusion MRI scans with both ASL and DSC techniques, and a T1 weighted and T2 weighted structural scan. A neuroradiologist (HAR) reviewed all structural MRI images to identify brain abnormalities that might exclude subjects from the statistical analyses. One subject from the control group did not receive the complete imaging protocol and was excluded. The detailed baseline demographic and clinical data on the remaining 15 subjects are listed in Table 1. None of them shows any group difference.

Recognition Memory Task

The fMRI paradigm consisted of an event-related task involving episodic recognition of neutral faces. Similarly designed paradigms in healthy adults evoke activation in medial and superior lateral parietal regions (Rugg and Henson, 2001), which are known to be vulnerable to pathological changes associated with AD (Buckner et al., 2005).

Stimuli—The stimuli for this task were gray scale photographs of neutral faces, taken from three stimulus sets: the Karolinska Directed Emotional Faces (KDEF) (Lundqvist, 1998), the AR Face Database (Martinez and Benavente, 1998), and the Nottingham Face Database (http://pics.psych.stir.ac.uk/). All faces were 280 × 280 pixel arrays centered on an 800×600 black screen, with an equal number of male and female neutral faces. All faces were looking straight ahead with eyes on the viewer. The stimuli were presented using Presentation software V10.3 (NeuroBehavioral Systems Inc).

Training session (encoding)—Thirty to forty minutes prior to the fMRI scan, participants underwent two sequentially-presented counterbalanced training sessions during which they viewed serially presented faces on a computer outside of the MRI scanner. Each training session consisted of 24 different faces each presented six times over the session. Faces were presented every 4 seconds. The stimulus repetition onset asynchrony averaged 12.6 s. The participants

were exposed to 48 different faces over the complete course of training. In a general set of training instructions, participants were told to view each sequentially-presented face, respond with a key press regarding likeability or age of the face, and try to remember each face as they may see the faces again as part of a memory task in the MRI scanner.

Functional MRI task—The task involved viewing previously-learned faces from the training sets as well as novel faces that had the same picture dimensions, male/female composition, grayscale coloring, neutral expressions, and forward-facing positioning. An event-related paradigm was used in which faces were presented for 2.2 seconds duration with an average stimulus onset asynchrony of 6.8 s (range 4–11s). In each of two scanning runs, 48 faces were presented in a pseudorandom order: 24 previously viewed (PV) faces from the training sessions and 24 novel (NV) faces. Participants maintained the same cognitive set throughout the experiment, which was to decide if the face was PV or whether it was NV. A white crosshair with a black background was presented during the variable length ISI. Responses to PV and NV faces were made with a two-button response device held in the right hand. The participants were instructed to use their index finger to identify PV faces and their middle finger for NV faces. All responses were recorded throughout the experiments. A single fMRI scan lasted 5 m 34 s and there were a total of two sequential iterations of the task for each subject (order was counterbalanced across participants). All faces were presented only once using back projection to a screen at the end of the scanner table with a computer-controlled projector (Dell 2300) in the scanner room. The presentation computer and the scanner were synchronized with a coaxial cable using MR scanner's TTL pulse so that scanner and task started at the same time. This also allowed synchronization between scan acquisition at each slice and stimulus delivery.

MR scanning protocol

Participants were provided with instruction and practice prior to scanning. All MR images were acquired on a GE 3.0T Signa whole body MRI scanner (General Electric, Milwaukee, WI) with an 8-channel head coil. The subject's head was constrained by foam padding.

fMRI image acquisition—A gradient recalled echo type echo-planar imaging (GRE-EPI) pulse sequence was used with higher order shimming applied to the static magnetic field (B_0). The EPI parameters were as follows: echo time = 30 ms; repetition time (TR) = 2000 ms; flip angle = 90°; acquisition matrix = 64×64; field of view (FOV) = 240 mm. Thirty continuous 4.5-mm-thick sagittal slices were acquired within each TR. Voxel resolution was 3.75 mm×3.75 mm×4.5 mm. Each fMRI scan collected 165 temporal volume images, of which the initial 3 image volumes of each scan were discarded. Following the functional scans, a T1 weighted three-dimensional, spoiled gradient-recalled at steady-state (SPGR) scan (TE/TR = 5 ms/24 ms, 40° flipangle, slice thickness = 1.2 mm, FOV = 240 mm, matrix= 256 × 192) and T2 weighted 3D Fast spin echo extended echo-train acquisition (3D-XETA) anatomic images (248 continuous sagittal slices, 1.2-mm slicethickness, TE/TR = 89 ms/2.5 s, FOV = 240 mm, matrix = 256 × 256) were acquired and later viewed by a neuroradiologist (HAR) for abnormalities that were inconsistent with the diagnosis and/or required clinical follow-up (none were found).

Arterial Spin Labeling (ASL) Perfusion image acquisition—ASL was performed using background suppressed continuous arterial spin labeling (Garcia et al., 2005b) with a stack of variable density spiral readout. To minimize blurring, the spiral acquisition was very short, just 4 ms, and the required resolution was achieved with 8 interleaves. Images were acquired at a 48×64×48 on an 18×24×18 cm FOV. The sequence employed repeated selective saturation of the slab at 4.3 s before imaging, a slab selective inversion at 3 s before imaging, continuous labeling from 3 s to 1.5 s before labeling, and nonselective inversion at 1.5 s, 764 ms, 334 ms, and 84 ms before imaging. The saturation and inversion were used to reduce the

background signal from the static spins to less than 2 % of normal, which greatly reduced motion artifact and the dynamic range requirements for whole brain 3D imaging. Continuous labeling was performed with a modification of a published (Alsop and Detre, 1998) method for multi-slice spin labeling with a single coil that virtually eliminates off-resonance errors. A labeling RF amplitude of 0.24 mG and a gradient amplitude of 1.6 mT/m were employed. Three ASL averages required just 5 minutes. Following the three ASL averages, an image was acquired with the same imaging sequence but with inversion recovery preparation instead of ASL. Saturation at 4.3s and then an inversion at 1650 ms before imaging was used to create a fluid suppressed image.

Dynamic Susceptibility Contrast (DSC) perfusion—In order to determine the dynamic cerebral perfusion information such as mean transit time (MTT) map, DSC images were acquired with a GRE-EPI sequence with the following parameters: TR/TE/ip angle: 2 s/28.4 ms/60°, 128×64 in-plane matrix over a 22×22 cm^2 FOV covering the whole brain in 15–18 7-mm-thick axial slices with 2 mm gaps. Data were acquired with a bolus injection of 0.1 mmol/kg Gadodiamide (Omniscan, Princeton, NJ). A time series of 36 images for each slice were acquired.

Image Processing and Data Analysis

BOLD fMRI—All fMRI EPI data were first slice-time corrected and motion corrected to the first volume image of the first time series using the Analysis of FunctionalNeuroImages (AFNI) software prior to subsequent processing in SPM5. In SPM5, the first EPI volume image from the time series was used for estimation of the normalization to the Montreal Neurological Institute (MNI) Echo-Planar Image (EPI) template using a 12 parameter affine transformation and 4×5×5 nonlinear basis function. With the resulting parameters, all the beta and contrast images from the regression analysis were normalized to the 2×2×2 mm imaging matrix and then spatially smoothed with an 8 mm full-width half-maximum (FWHM) Gaussian filter.

For individual subject analyses, a fixed effects event-related design with multiple linear regression time series analyses was used to determine the location and extent of brain activations. The hemodynamic response function (HRF) used to analyze each participant's time series data was modeled in SPM5 and included two gamma functions of the canonical HRF and a temporal derivative term.. The latency images of the canonical HRF for the PV stimuli were calculated using β_1 and β_2 images according to the original equation from Henson et al.: Latency = 3.56 s/(1+ exp $(3.1*\beta_2/\beta_1)) - 1.78$ s, where β_1 is the HRF parameter estimate and β_2 is the temporal derivative estimate (Henson et al., 2002).

The BOLD contrast PV > NV was computed from the HRF parameter estimates for each subject, normalized to the MNI template and subsequently entered into second-level random effect analyses. An omnibus *F*-test was computed in order to determine the brain regions where the canonical HRF provided a reasonable fit to the data. The treatment group was compared to the placebo group using a two-sample t-test constrained within the voxels that were active to the task. This was accomplished by using the functional map of the task effect, ($p<0.05$, uncorrected) as an explicit mask in the two-sample t-test and brain areas of difference were identified at the voxel level for $p < 0.005$ (uncorrected) and the cluster extend size >750 voxels, resulting in a cluster-corrected threshold of $p < 0.05$ (Alphasim, AFNI) within the omnibus F mask of the overall task activation.

Perfusion images

ASL quantitative CBF (qCBF) image

Each individual ASL image was generated by averaging the pair-wise subtraction of tagging/control images. For quantification of flow, a low resolution sensitivity map for water sensitivity is required. This was created from the fluid suppressed image, which showed essentially no contrast between gray and white matter. We used a local maximum operator on the image and treated all tissue signals as white matter with a water concentration of 0.735 gm/ml (Herscovitch and Raichle, 1985) and a T1 of 900ms. Assuming gray matter with a water concentration of 0.88 gm/ml and a T1 of 1150 caused only a 5% calibration difference. This calibration produced a sensitivity map, C, equal to the fully relaxed MRI signal intensity produced by one gm of water per ml of brain. With this coregistered sensitivity map C, cerebral blood flow (CBF) was calculated using the equation:

$$CBF=\frac{\rho_b(S_c - S_l)}{2\alpha C\omega_a T1_a \exp\left(-\frac{w}{T1_a}\right)\left(1-\exp\left(-\frac{tl}{T1_a}\right)\right)}$$

where ρ_b is the density of brain tissue, 1.05g/ml(Herscovitch and Raichle, 1985) α is the labeling efficiency, assumed to be 95% for labeling times 75% for background suppression (Garcia et al., 2005a), w is the postlabeling delay(Alsop and Detre, 1996), 1.5s, tl is the labeling duration, 1.5s, $T1_a$ is the T1 of arterial blood, ω_a is the density of water in blood, 0.85 g/ml (Herscovitch and Raichle, 1985), and S_l and S_c are the signal intensities in the labeled and control images, respectively. This equation assumes that the labeled blood remains in the arterioles and capillaries and does not reach the tissue. All the ASL-qCBF images were then normalized to the standard MNI positron emission tomography (PET) perfusion image template (2×2×2mm imaging matrix) in SPM5 with the modulation method to preserve the intensity of CBF values. Grey matter and white matter templates from the standard SPM MNI templates were used to calculate the global perfusion rates among all the subjects. A voxel-wise comparison of CBF images between statin group and placebo did not find any significant cluster with group threshold $p< 0.05$ (voxel level $p<0.005$ & cluster size > 750 voxels).

DSC Perfusion analysis

The dynamic perfusion images were processed as follows. Gadolinium concentration as a function of time (Rosen et al., 1990), $C(t)$, was determined K ($S(t)$) for each voxel using the Equation: $C(t)= -\frac{K}{TE}\ln\left(\frac{S(t)}{S_0}\right)$, where $S(t)$ is the corresponding signal intensity at time t after injection, S_0 is the pre-injection signal, TE is the echo time, and K reflects the contrast agent relaxivity and properties of the pulse sequence. The arterial input function (AIF) was automatically selected based on early arrival time, large signal change, and fast passage of the MR contrast (Carroll et al., 2003). A deconvolution method (Ostergaard et al., 1996) that is insensitive to delay of contrast arrival in the tissue (Wu et al., 2003) was used to deconvolve the AIF from $C(t)$ in order to obtain CBV_{DSC} and CBF_{DSC} on a voxel-by-voxel basis for all slices. The cerebral blood mean transit time (MTT) was calculated with the central volume principle: MTT = CBV/CBF. The final MTT maps were then normalized to the standard MNI image template (2×2×2mm imaging matrix) in SPM5 with the modulation method.. A voxel-wise comparison of MTT images between statin group and placebo did not find any significant cluster with group threshold $p< 0.05$ (voxel level $p<0.005$ & cluster size > 750 voxels).

Results

Behavioral results

Accuracy and reaction times are presented in Table 2. Analysis of variance and post-hoc comparisons revealed that both groups performed the recognition memory task with accuracy above 80%. The treatment group and placebo group did not differ on overall accuracy or reaction time to NV and PV faces during both training session and fMRI experiments. Mini Mental State Exam (MMSE) scores were also equivalent between groups.

Imaging results

Group averaged CBF from all subjects shown in Fig. 1A captured the quality of the current MR cerebral perfusion images with ASL technique. In Fig. 1B, the BOLD group activation map from all the participants (n=15) (Group level $p<0.05$ correction for multiple comparisons) showed bilateral activation of the superior temporal gyrus and inferior parietal lobule, bilateral posterior cingulate cortices, right superior frontal sulcus and postcentral gyrus.

Hemodynamic canonical amplitude and cerebral blood flow comparison

Fig. 2A depicts the cerebral hemodynamic response difference to PV faces versus NV faces. The BOLD signal amplitude from the atorvastatin group was significantly greater than the placebo group in the middle and superior frontal gyrus, superior temporal gyrus, bilateral posterior cingulate gyrus and precuneus. Coordinates and statistics for these regional BOLD signal changes are listed in Table 3. Since BOLD signal change could be affected by the resting cerebral perfusion level, the quantitative resting CBF (qCBF) values measured by the ASL technique were also extracted from the above areas. As shown in Fig. 2. B for the right angular gyrus, BOLD amplitude signal changes were 0.265 ± 0.1 % (mean±SE) from the statin group and −0.19 ± 0.06 % (mean±SE) in the placebo group ($p<0.005$, Wilcoxon non-parametric test). However, qCBF values from the same areas were 74.6 ± 10.4 (mean±SE) ml/100g/min for the statin group and 54.3 ± 10.4 (mean±SE) ml/100g/min for placebo group. Differences in qCBF values were not significant ($p<0.30$, Wilcoxon non-parametric test) between the two groups. Neither global grey matter nor white matter perfusion rate showed significant difference due to the group effect. A detailed comparison is listed in Table 3. In Fig. 2.C, in right angular gyrus, the BOLD contrast signal (PV vs. NV) shows a strong linear correlation (cc=0.56) with the resting CBF values across all the subjects. However, the correlation interaction with group is not significant ($p<0.824$) as tested by the parallelism with nonparametric Sen-Adichie method in Table 3.

Canonical hemodynamic response latency and cerebral perfusion mean transit time comparison

The cerebral hemodynamic response latency difference due to the treatment effect is depicted in Fig. 3. During recognition of PV faces, the latencies in the bilateral cuneus and precuneus, left precentral gyrus and cingulate cortex were significantly faster in the treatment group compared to the placebo group (Fig. 3A). The resting perfusion mean transit times from these areas were extracted and no treatment effect was found between the groups. Details regarding the coordinates, statistics and regional BOLD response latency values and MTT values are listed in Table 3. In Fig. 3.B, the regional BOLD response latency values from the right cuneus area are plotted with the MTT values, showing that, while MTT values remain similar between groups, the hemodynamic response latency was faster in the statin treated group than in the placebo group. The averaged BOLD hemodynamic response function time course further depicts the earlier peak response in the statin group (Fig. 3. C).

Discussion

This report combines the use of fMRI BOLD signal change both in amplitude and latency with resting perfusion measurements to assess the effect of drug intervention in asymptomatic persons at risk for AD. To date, most AD-related fMRI research has focused almost exclusively on comparisons of the amplitude of BOLD signal, with the exception of a study by Rombouts et al. that reported delayed rather than decreased BOLD response as marker for early Alzheimer's disease (Rombouts et al., 2005). In that study, different phases of the BOLD response were analyzed by orthogonal regressors and AD patients showed increased delay of BOLD response comparing to normal controls. This study stressed the importance of analyzing BOLD signal with temporal characteristic parameters in AD studies. However, this method has not been further adopted in AD related neuroimaging study mainly because it is susceptible to the high variations within the BOLD temporal signal and ambiguity of manual selection of the BOLD phase. However, latency changes that are derived from the temporal derivative of the BOLD signal do not require a predefined BOLD phase. Therefore, this method is useful for providing an estimation of temporal information about the BOLD signal source as it relates to the disease process or drug treatment effect. In this study, fMRI BOLD activation signals showed greater amplitude and shorter latency of hemodynamic response in subjects who received statin treatment compared to those in the placebo group. The BOLD signal is purported to be tightly correlated with underlying neuronal activity (Logothetis et al., 2001), the signal itself depends on the blood-flow mediated relationship between neural activity and focal paramagnetic deoxygenated hemoglobin concentration (Davis et al., 1998). Although the possible statin effects on changing cerebral neuronal activity could not be ruled out, atorvastatin used in the current study does not pass the blood-brain-barrier well and its direct effect on modifying neuronal activities is limited. The equivalent performance during the recognition task suggests that the measured group differences in BOLD signal strength and latency are not a function of differences in task difficulty or cognitive status in these asymptomatic cognitively healthy adults. These greater and faster BOLD signals in the drug-treated group may reflect differences in neurovascular coupling changes due to statin's effect on endothelial function. Globally-scaled cerebral perfusion measurements with either qCBF or MTT showed no significant difference between groups in this regionally focused cross-sectional analysis. Other analyses from these data are underway to determine whether statin treatment results in changes in cerebral perfusion from the pre-treatment baseline scan.

Statins exhibit pleiotropic effects that lead to not only clear cardiovascular benefits, but also to possible protection against neurodegenerative diseases such as AD. Clinical trials show that statins lower serum cholesterol, improve endothelial function, and reduce inflammation – factors that may improve cerebral perfusion and, thus, protect against neurodegeneration. In addition, statins may also modify β-amyloid deposition and metabolism in the brain, a pathologic hallmark of AD progression (Fassbender et al., 2001; Simons et al., 2001). While some mechanisms of disease may be slower to respond to statin therapy, statins acutely upregulate endothelial nitric oxide (NO) synthase, leading to increased NO availability, rapid improvement in endothelial function, and improved CBF (O'Driscoll et al., 1997; Yamada et al., 2000). The BOLD signal changes seen in the statin treated group in the present study could be due to the cellular regulation of NO, an important soluble mediator of neurovascular coupling. These improvements may result in a tighter relationship of neurovascular coupling and cause stronger and faster BOLD signal upon neuronal activities. These findings might have potential therapeutic implications for various neurological disorders, including stroke, AD, Parkinson's disease, and multiple sclerosis. While previous studies have not evaluated statin effects on the cerebral microvasculature perfusion using ASL-MRI or DSC-MRI, some analyses of large vessel CBF using transcranial Doppler or other MRI perfusion techniques have shown mixed results (Pretnar-Oblak et al., 2006; ten Dam et al., 2005). As changes in small vessel vasoreactivity may have a greater impact on the development of cognitive decline

in AD compared to large vessel disease, larger randomized, controlled studies investigating the effects of statins on microvascular changes in CBF and functional activation are needed to clarify the potential role of statins in prevention of cognitive decline and AD.

Although there was no significant group difference in CBF, the mean qCBF estimates for the statin treated subjects are consistently higher than those for the placebo treated subjects. Given the small sample sizes for the current study, low power in the present analysis may confound the significance of flow change due to statin treatment effect. The dynamic of BOLD response is related to the perfusion level in that the BOLD response is faster during elevated CBF and slower during diminished CBF (Friston et al., 2000). In the current study, the shorter latency of BOLD response in statin group may relate to the slightly elevated perfusion rate. Furthermore, a positive correlation between baseline perfusion estimated by qCBF and BOLD magnitude contrast signal was found across all the subjects in the right angular gyrus. In contrast to our findings, results of a hypercapnia study showed that with increased CBF, the BOLD response was lower in amplitude and more latent (Cohen et al. 2002). Such a discrepancy in findings may be related to the different drugs effect on the cerebral vasculature (statin vs. CO_2), activated focal brain areas (parietal vs. occipital cortexes), type of stimuli used (cognitive memory task vs. visual stimuli), and most importantly, the difference in arterial vascular resistance and the dynamic autoregulatory response of brain tissue (hypercapnia vs. normal physiological conditions).

There are several limitations to the current study. The cross-sectional nature of this analysis limits our ability to comment on a causal relationship between statin use and BOLD signal amplitude and response latencies. However, the goal of this analysis was to generate hypotheses to be tested in larger prospective clinical trials integrating treatments with fMRI outcome measures. The small sample size of this pilot study may have led to bias by the limited SNR of the neuroimaging signal. In addition, because of the limited sample size, the present analyses were restricted to voxels in which the canonical HRF provided a reasonable fit to the data with a relatively lenient threshold ($P<0.05$, uncorrected). The latency calculated by the Henson et al. method is limited by the approximation level of the canonical HRF to the real BOLD impulse response. The different temporal characteristics and amplitudes of the hemodynamic responses between the two groups raise the question of whether applying the same HRF model in both groups is a valid approach. In addition, according to Calhoun's analysis of latency-induced amplitude bias (Calhoun et al., 2004), the statin treated subjects' BOLD signal amplitude could have been underestimated when their hemodynamic responses peaked earlier than the 6 s peak in the canonical HRF. However, this would be expected to contribute to even greater differences between the two groups than reported here. During the ASL perfusion quantification, several constants and assumptions had been made such as the blood T1 value and ASL tagging pulse efficiency. Although these variables are less likely to be affected by the statin treatment effect, it would bring uncertainty into the results.

Finally, since statins are one of the most frequently-prescribed classes of prescription drugs among the middle-aged and elderly populations, researchers should be mindful when designing studies and selecting subjects that statin therapy may have an effect on BOLD signal.

Conclusion

In this cross-sectional analysis of subjects treated with 4 months of atorvastatin therapy vs. placebo, we have shown stronger and faster BOLD signal in statin treated subjects compared to placebo treated subjects during a recognition memory task, while the resting CBF and MTT values from the same regions remained similar between groups. The atorvastatin group's greater BOLD response may suggest improvement of cerebral vasoreactivity, possibly due to the statin's effect on neurovascular coupling or the neuronal activity itself. In addition, the fact

that these differences in BOLD characteristics did not coincide with differences in qCBF or MTT values between groups suggests that the hemodynamic response may not be a simple consequence of the baseline perfusion rate changes. Larger randomized controlled studies assessing the effects of statins on small vessel CBF, fMRI activation, and cognitive outcomes are underway in persons at risk for AD. The direct comparison of the amplitude of BOLD responses typical of most fMRI research on AD is limited when applied in the absence of other measures of signal time course or vascular function. The current study provides a model for addressing this limitation by combining an analysis of signal amplitude and signal latency with resting perfusion rates. Future studies of this kind could help to characterize the fMRI signal and its relation to the compromised perfusion rate in AD risk population. Futhermore, given the statin effect on manipulating the HRF on these healthy middle-aged or older adults, future experiment design of such fMRI studies might need to consider statin usage in the inclusion criteria.

Acknowledgments

This study was supported by a Wisconsin Comprehensive Memory Program Alzheimer's Disease Pilot Study Award with funds from the State of Wisconsin and the University of Wisconsin General Clinical Research Center (NCRR grant M01 RR03186). Dr. Carlsson was supported by a Beeson Career Development Award (1K23 AG026752-01, a grant jointly funded by NIA, the John A. Hartford Foundation, Atlantic Philanthropies, and the Starr Foundation). Portions of this study were supported by the NIA (R01 AG21155) and a Merit Review Grant from the Department of Veterans Affairs. The authors would like to sincerely thank all of the dedicated research participants. This is Madison VA GRECC manuscript number # 2007-11.

References

Alsop DC, Detre JA. Reduced transit-time sensitivity in noninvasive magnetic resonance imaging of human cerebral blood flow. J Cereb Blood Flow Metab 1996;16:1236–1249. [PubMed: 8898697]

Alsop DC, Detre JA. Multisection cerebral blood flow MR imaging with continuous arterial spin labeling. Radiology 1998;208:410–416. [PubMed: 9680569]

Bookheimer SY, Strojwas MH, Cohen MS, Saunders AM, Pericak-Vance MA, Mazziotta JC, Small GW. Patterns of brain activation in people at risk for Alzheimer's disease. N Engl J Med 2000;343:450–456. [PubMed: 10944562]

Braak H, Braak E. Neuropathological stageing of Alzheimer-related changes. Acta Neuropathol (Berl) 1991;82:239–259. [PubMed: 1759558]

Buckner RL, Snyder AZ, Shannon BJ, LaRossa G, Sachs R, Fotenos AF, Sheline YI, Klunk WE, Mathis CA, Morris JC, Mintun MA. Molecular, structural, and functional characterization of Alzheimer's disease: evidence for a relationship between default activity, amyloid, and memory. J Neurosci 2005;25:7709–7717. [PubMed: 16120771]

Calhoun VD, Stevens MC, Pearlson GD, Kiehl KA. fMRI analysis with the general linear model: removal of latency-induced amplitude bias by incorporation of hemodynamic derivative terms. Neuroimage 2004;22:252–257. [PubMed: 15110015]

Carroll TJ, Rowley HA, Haughton VM. Automatic calculation of the arterial input function for cerebral perfusion imaging with MR imaging. Radiology 2003;227:593–600. [PubMed: 12663823]

Cohen ER, Ugurbil K, Kim SG. Effect of basal conditions on the magnitude and dynamics of the blood oxygenation level-dependent fMRI response. J Cereb Blood Flow Metab 2002;22:1042–1053. [PubMed: 12218410]

D'Esposito M, Zarahn E, Aguirre GK, Rypma B. The effect of normal aging on the coupling of neural activity to the bold hemodynamic response. Neuroimage 1999;10:6–14. [PubMed: 10385577]

Davis TL, Kwong KK, Weisskoff RM, Rosen BR. Calibrated functional MRI: mapping the dynamics of oxidative metabolism. Proc Natl Acad Sci U S A 1998;95:1834–1839. [PubMed: 9465103]

Dickerson BC, Salat DH, Greve DN, Chua EF, Rand-Giovannetti E, Rentz DM, Bertram L, Mullin K, Tanzi RE, Blacker D, Albert MS, Sperling RA. Increased hippocampal activation in mild cognitive impairment compared to normal aging and AD. Neurology 2005;65:404–411. [PubMed: 16087905]

Fassbender K, Simons M, Bergmann C, Stroick M, Lutjohann D, Keller P, Runz H, Kuhl S, Bertsch T, von Bergmann K, Hennerici M, Beyreuther K, Hartmann T. Simvastatin strongly reduces levels of Alzheimer's disease beta -amyloid peptides Abeta 42 and Abeta 40 in vitro and in vivo. Proc Natl Acad Sci U S A 2001;98:5856–5861. [PubMed: 11296263]

Fleisher AS, Houston WS, Eyler LT, Frye S, Jenkins C, Thal LJ, Bondi MW. Identification of Alzheimer disease risk by functional magnetic resonance imaging. Arch Neurol 2005;62:1881–1888. [PubMed: 16344346]

Friston KJ, Mechelli A, Turner R, Price CJ. Nonlinear responses in fMRI: the Balloon model, Volterra kernels, and other hemodynamics. Neuroimage 2000;12:466–477. [PubMed: 10988040]

Garcia D, Duhamel G, Alsop D. Efficiency of Inversion Pulses for Background Suppressed Arterial Spin Labeling. Magn Reson Med 2005a;54:366–372. [PubMed: 16032674]

Garcia DM, Duhamel G, Alsop DC. Efficiency of inversion pulses for background suppressed arterial spin labeling. Magn Reson Med 2005b;54:366–372. [PubMed: 16032674]

Haxby JV, Ungerleider LG, Horwitz B, Maisog JM, Rapoport SI, Grady CL. Face encoding and recognition in the human brain. Proc Natl Acad Sci U S A 1996;93:922–927. [PubMed: 8570661]

Henson RN, Price CJ, Rugg MD, Turner R, Friston KJ. Detecting latency differences in event-related BOLD responses: application to words versus nonwords and initial versus repeated face presentations. Neuroimage 2002;15:83–97. [PubMed: 11771976]

Herscovitch P, Raichle ME. What is the correct value for the brain--blood partition coefficient for water? J Cereb Blood Flow Metab 1985;5:65–69. [PubMed: 3871783]

Hoge RD, Atkinson J, Gill B, Crelier GR, Marrett S, Pike GB. Linear coupling between cerebral blood flow and oxygen consumption in activated human cortex. Proc Natl Acad Sci U S A 1999;96:9403–9408. [PubMed: 10430955]

Johnson SC, Schmitz TW, Moritz CH, Meyerand ME, Rowley HA, Alexander AL, Hansen KW, Gleason CE, Carlsson CM, Ries ML, Asthana S, Chen K, Reiman EM, Alexander GE. Activation of brain regions vulnerable to Alzheimer's disease: the effect of mild cognitive impairment. Neurobiol Aging 2006a;27:1604–1612. [PubMed: 16226349]

Johnson SC, Schmitz TW, Trivedi MA, Ries ML, Torgerson BM, Carlsson CM, Asthana S, Hermann BP, Sager MA. The influence of Alzheimer disease family history and apolipoprotein E epsilon4 on mesial temporal lobe activation. J Neurosci 2006b;26:6069–6076. [PubMed: 16738250]

Kivipelto M, Helkala EL, Laakso MP, Hanninen T, Hallikainen M, Alhainen K, Iivonen S, Mannermaa A, Tuomilehto J, Nissinen A, Soininen H. Apolipoprotein E epsilon4 allele, elevated midlife total cholesterol level, and high midlife systolic blood pressure are independent risk factors for late-life Alzheimer disease. Ann Intern Med 2002;137:149–155. [PubMed: 12160362]

Laurienti PJ, Field AS, Burdette JH, Maldjian JA, Yen YF, Moody DM. Relationship between caffeine-induced changes in resting cerebral perfusion and blood oxygenation level-dependent signal. AJNR Am J Neuroradiol 2003;24:1607–1611. [PubMed: 13679279]

Logothetis NK, Pauls J, Augath M, Trinath T, Oeltermann A. Neurophysiological investigation of the basis of the fMRI signal. Nature 2001;412:150–157. [PubMed: 11449264]

Lundqvist D, Litton JE. The Averaged Karolinska Directed Emotional Faces - AKDEF. 1998

Martinez AM, Benavente R. The AR Face Database. 1998 CVC Technical Report #24.

Masse I, Bordet R, Deplanque D, Al Khedr A, Richard F, Libersa C, Pasquier F. Lipid lowering agents are associated with a slower cognitive decline in Alzheimer's disease. J Neurol Neurosurg Psychiatry 2005;76:1624–1629. [PubMed: 16291883]

McKhann G, Drachman D, Folstein M, Katzman R, Price D, Stadlan EM. Clinical diagnosis of Alzheimer's disease: report of the NINCDS-ADRDA Work Group under the auspices of Department of Health and Human Services Task Force on Alzheimer's Disease. Neurology 1984;34:939–944. [PubMed: 6610841]

Miezin FM, Maccotta L, Ollinger JM, Petersen SE, Buckner RL. Characterizing the hemodynamic response: effects of presentation rate, sampling procedure, and the possibility of ordering brain activity based on relative timing. Neuroimage 2000;11:735–759. [PubMed: 10860799]

O'Driscoll G, Green D, Taylor RR. Simvastatin, an HMG-coenzyme A reductase inhibitor, improves endothelial function within 1 month. Circulation 1997;95:1126–1131. [PubMed: 9054840]

Ogawa S, Lee TM, Kay AR, Tank DW. Brain magnetic resonance imaging with contrast dependent on blood oxygenation. Proc Natl Acad Sci U S A 1990;87:9868–9872. [PubMed: 2124706]

Ostergaard L, Weisskoff RM, Chesler DA, Gyldensted C, Rosen BR. High resolution measurement of cerebral blood flow using intravascular tracer bolus passages. Part I: Mathematical approach and statistical analysis. Magn Reson Med 1996;36:715–725. [PubMed: 8916022]

Petersen RC, Smith GE, Waring SC, Ivnik RJ, Kokmen E, Tangelos EG. Aging, memory, and mild cognitive impairment. Int Psychogeriatr 9 Suppl 1997;1:65–69.

Petrella JR, Coleman RE, Doraiswamy PM. Neuroimaging and early diagnosis of Alzheimer disease: a look to the future. Radiology 2003;226:315–336. [PubMed: 12563122]

Pretnar-Oblak J, Sabovic M, Sebestjen M, Pogacnik T, Zaletel M. Influence of atorvastatin treatment on L-arginine cerebrovascular reactivity and flow-mediated dilatation in patients with lacunar infarctions. Stroke 2006;37:2540–2545. [PubMed: 16931784]

Rombouts SA, Goekoop R, Stam CJ, Barkhof F, Scheltens P. Delayed rather than decreased BOLD response as a marker for early Alzheimer's disease. Neuroimage 2005;26:1078–1085. [PubMed: 15961047]

Rosen BR, Belliveau JW, Vevea JM, Brady TJ. Perfusion imaging with NMR contrast agents. Magn Reson Med 1990;14:249–265. [PubMed: 2345506]

Rother J, Knab R, Hamzei F, Fiehler J, Reichenbach JR, Buchel C, Weiller C. Negative dip in BOLD fMRI is caused by blood flow--oxygen consumption uncoupling in humans. Neuroimage 2002;15:98–102. [PubMed: 11771977]

Rugg, MD.; Henson, RN. Cognitive Neuroscience of Memory Encoding and Retrieval. Psychology Press; London: 2001.

Sager MA, Hermann B, La Rue A. Middle-aged children of persons with Alzheimer's disease: APOE genotypes and cognitive function in the Wisconsin Registry for Alzheimer's Prevention. J Geriatr Psychiatry Neurol 2005;18:245–249. [PubMed: 16306248]

Simons M, Keller P, Dichgans J, Schulz JB. Cholesterol and Alzheimer's disease: is there a link? Neurology 2001;57:1089–1093. [PubMed: 11571339]

Smith CD, Andersen AH, Kryscio RJ, Schmitt FA, Kindy MS, Blonder LX, Avison MJ. Altered brain activation in cognitively intact individuals at high risk for Alzheimer's disease. Neurology 1999;53:1391–1396. [PubMed: 10534240]

ten Dam VH, Box FM, de Craen AJ, van den Heuvel DM, Bollen EL, Murray HM, van Buchem MA, Westendorp RG, Blauw GJ. Lack of effect of pravastatin on cerebral blood flow or parenchymal volume loss in elderly at risk for vascular disease. Stroke 2005;36:1633–1636. [PubMed: 16049200]

Trivedi MA, Schmitz TW, Ries ML, Torgerson BM, Sager MA, Hermann BP, Asthana S, Johnson SC. Reduced hippocampal activation during episodic encoding in middle-aged individuals at genetic risk of Alzheimer's disease: a cross-sectional study. BMC Med 2006;4:1. [PubMed: 16412236]

Wu O, Ostergaard L, Koroshetz WJ, Schwamm LH, O'Donnell J, Schaefer PW, Rosen BR, Weisskoff RM, Sorensen AG. Effects of tracer arrival time on flow estimates in MR perfusion-weighted imaging. Magn Reson Med 2003;50:856–864. [PubMed: 14523973]

Yamada M, Huang Z, Dalkara T, Endres M, Laufs U, Waeber C, Huang PL, Liao JK, Moskowitz MA. Endothelial nitric oxide synthase-dependent cerebral blood flow augmentation by L-arginine after chronic statin treatment. J Cereb Blood Flow Metab 2000;20:709–717. [PubMed: 10779015]

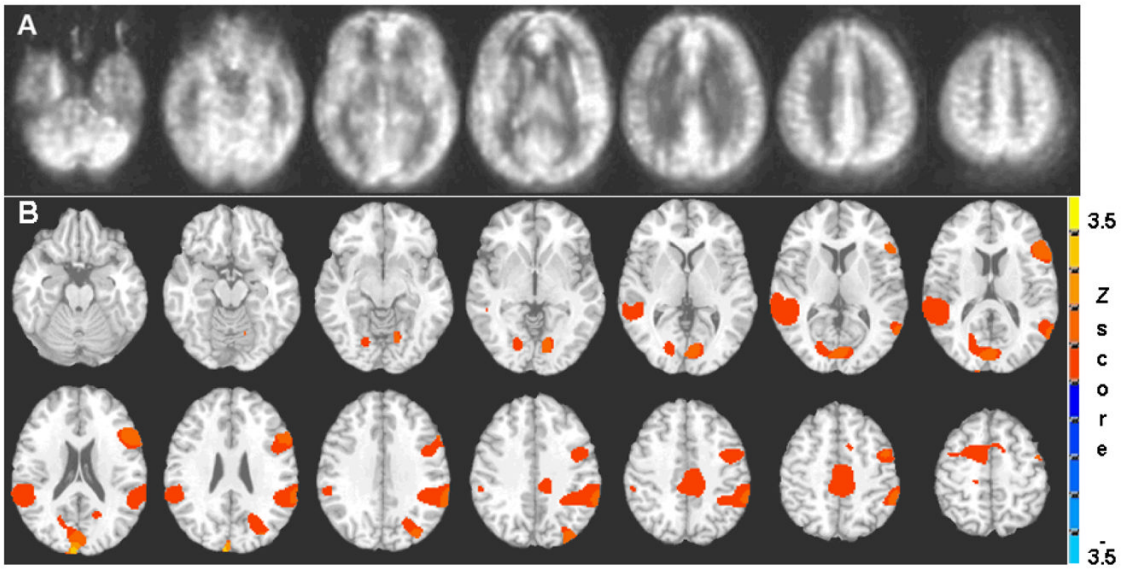

Figure 1.
Group averaged cerebral blood flow (CBF) maps from all subjects (n=15) shows the quality of the quantitative perfusion images using arterial spin labeling technique (A). The BOLD fMRI group activation map (B) for PV > NV *(p<0.05 corrected for multiple comparisons)* shows bilateral activation of the superior temporal gyrus and inferior parietal lobule, bilateral posterior cingulate cortices, right superior frontal sulcus and postcentral gyrus.

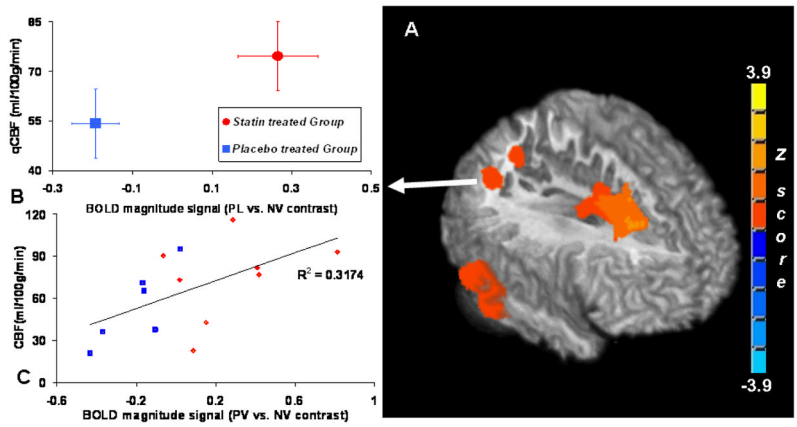

Figure 2.

3D-Surface rendering with middle sagittal view (A) of the significant areas in two sample t-tests where the statin treated group shows significantly greater BOLD canonical signal change than the placebo treated group during the face recognition task (PV > NV) in the right prefrontal and superior frontal sulcus, right inferior parietal lobules, and right angular gyrus. The voxel based comparisons were limited to the brain areas activated by the memory task and a group level threshold $p<0.05$ (*voxel-level* threshold of $p<0.005$ was chosen with *cluster size correction* for multiple comparisons). (B). Group averaged BOLD signal change and resting qCBF values from the area of the right angular gyrus are plotted. (C). Scatter plot depicts the linear correlation (cross correlation coefficient = 0.56) between BOLD magnitude contrast signal (PV vs. NV) and the baseline CBF values at right angular gyrus across all the subjects in this study.

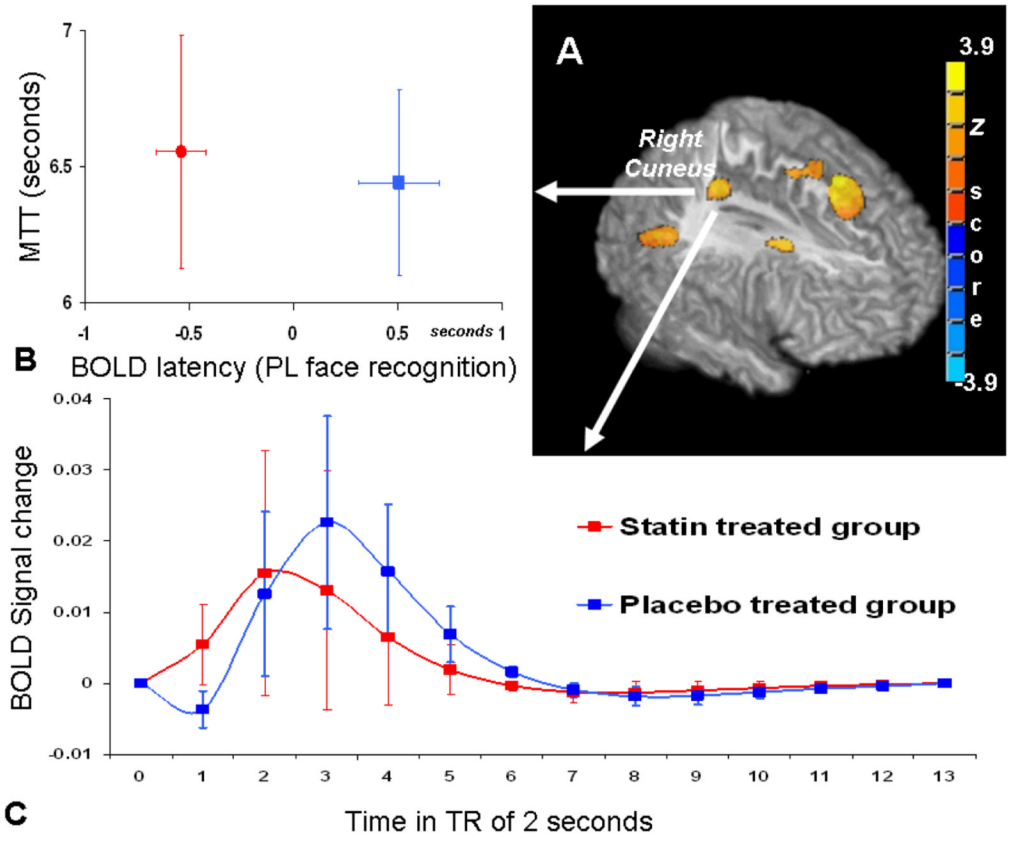

Figure 3.

3D rendering (A) of the significant areas in two sample t-tests where the statin treated group shows significantly faster hemodynamic signal change than the placebo treated group during the PV face recognition task. The group comparison threshold of $p<0.05$ ($p<0.005$ at voxel level with cluster size correction) was chosen, corrected for multiple comparisons and the analysis was restricted to the brain areas activated by the memory task. Within the right cuneus area, averaged BOLD latency values are plotted with the resting perfusion mean transit time (B); and the averaged BOLD hemodynamic response time course shows the BOLD signal peak from statin treated group occurs earlier than the placebo treated group (C).

Table 1

Demographic and clinical data at baseline

Characteristic (n=15)	**Value***
Age, y	52.1 ± 7.7
Education, y	15.8 ± 2.8
Women, n (%)	8 (62)
APOE4 carriers, n (%)	3 (23)
Total cholesterol, mg/dL	195.1 ± 41.7
HDL cholesterol, mg/dl	65.4 ± 20.9
LDL cholesterol, mg/dL	111.1 ± 32.6
Systolic blood pressure, mm Hg	125.5 ± 18.5
Body mass index (BMI), kg/m^2	27.5 ± 5.0
Diabetes mellitus, n (%)	0 (0)
Current tobacco use, n (%)	2 (13)

* All values are mean ± SD unless otherwise indicated.

Table 2

fMRI task performance and cognitive status data

	Statin Treated Subjects (n=8) (Mean ± SD)	**Placebo Treated Subjects (n=7) (Mean ± SD)**
Reaction time to faces during training session	1.20 ± 0.62 s	1.28 ± 0.56 s
Reaction time to PV faces (s) during fMRI scan	1.35 ± 0.38 s	1.36 ± 0.19 s
Reaction time to NV faces (s) during fMRI scan	1.22 ± 0.32 s	1.25 ± 0.11 s
Accuracy (%) of fMRI task	82.89 ± 20.07	85.89 ± 9.71
MMSE score	29.29 ± 0.76	29.50 ± 0.55

MMSE: Mini Mental Status Exam.

None of these parameters show any group difference.

Table 3

Effect of treatment on BOLD signal

	Cluster center	BOLD averaged amplitude signal (%)		P	qCBF		P	BOLD qCBF interaction
	x,y,z (mm)				(ml/100g/min)			
Description		Statin Treated Subjects (n=8) (Mean ± SE)	Placebo Treated Subjects (n=7) (Mean ± SE)	statin vs. Placebo *(P)	Statin Treated Subjects (n=8) (Mean ± SE)	Placebo Treated Subjects (n=7) (Mean ± SE)	statin vs. Placebo *(P)	statin vs. Placebo **
Right angular gyrus	46,−54,40	0.265 ± 0.1	−0.19 ± 0.06	0.005	74.6 ± 10.4	54.3 ± 10.4	0.30	P = 0.824
Right middle temporal gyrus	66, −32, −26	0.30 ± 0.06	−0.21 ± 0.10	0.005	53.6 ± 8.6	44.8 ± 6.7	0.16	P = 0.354
Left superior parietal lobule	−18, −70,46	0.45 ± 0.16	−0.19 ± 0.10	0.010	70.2 ± 10.8	55.0 ± 13.1	0.44	P = 0.202
Right superior frontal sulcus	20, −20,58	0.40 ± 0.12	−0.05 ± 0.04	0.014	45.6 ± 8.0	33.9 ± 6.3	0.30	P = 0.75
Global Grey Matter					62.0 ± 16.8	60.0 ± 10.7	0.875	N/A
Global white Matter					46.9 ± 11.8	45.4 ± 7.7	0.713	N/A
		BOLD latency to PV faces (s)			Cerebral Blood Mean Transit Time (s)			
Right middle frontal gyrus	30, −4,68	−0.40 ± 0.33	1.05 ± 0.12	0.008	5.68 ± 0.33	5.14 ± 0.19	0.29	N/A
Left precentral gyrus	−45, −5,24	−0.25 ± 0.16	1.02 ± 0.17	0.001	6.23 ± 0.39	6.22 ± 0.33	0. 73	N/A
Right posterior middle frontal gyrus	30, −7,43	−0.69 ± 0.12	0.65 ± 0.09	0.001	6.14 ± 0.40	6.09 ± 0.32	0.73	N/A
Left cuneus	−21, −62,18	−0.36 ± 0.21	0.87 ± 0.16	0.001	6.65 ± 0.39	6.35 ± 0.33	0.64	N/A

* Group difference in BOLD and ASL between groups were tested by non-parametric Wilcoxon rank test.

** Interactions of BOLD and ASL were tested by non-parametric Check Assumption of Parallelism (Sen, Adichie).